

A.A.Gusev

Current research on empirical trends and models of
earthquake source scaling

Petropavlovsk-Kamchatsky, RUSSIA

¹Institute of Volcanology and Seismology, FED, Russian Ac. Sci.

² Kamchatka Branch, Geophysical Service, Russian Ac. Sci.

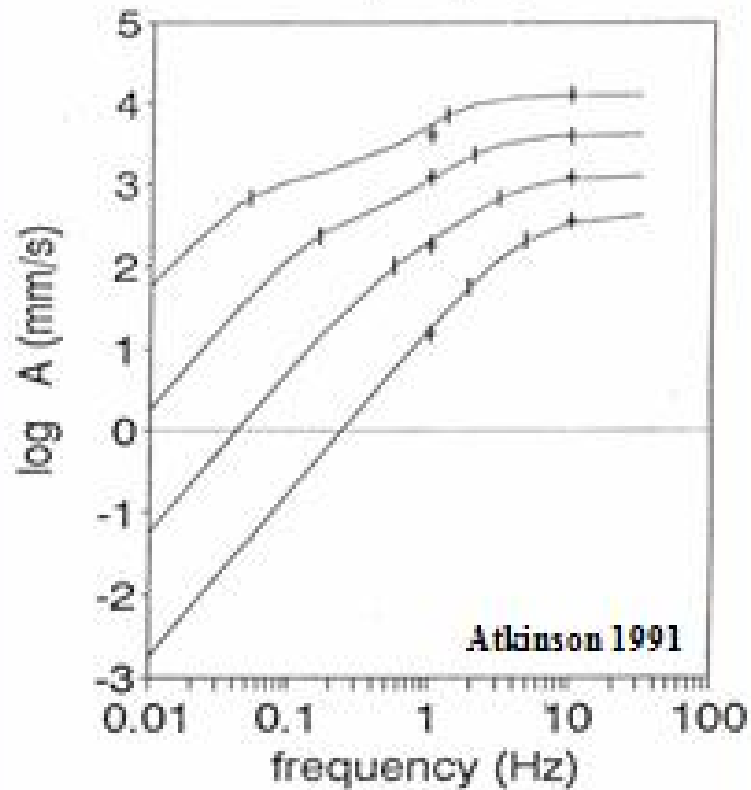
PART 1

Splitting f_{max} : separating site-controlled and source-controlled contributions
into the upper cutoff of acceleration spectrum
of a local earthquake

(A.A Gusev, E.M.Guseva 2015).

Empirical scaling laws for FSA, with f_{c2} feature

ENA Model
 $M = 4, 5, 6, 7$



W.U.S.A model

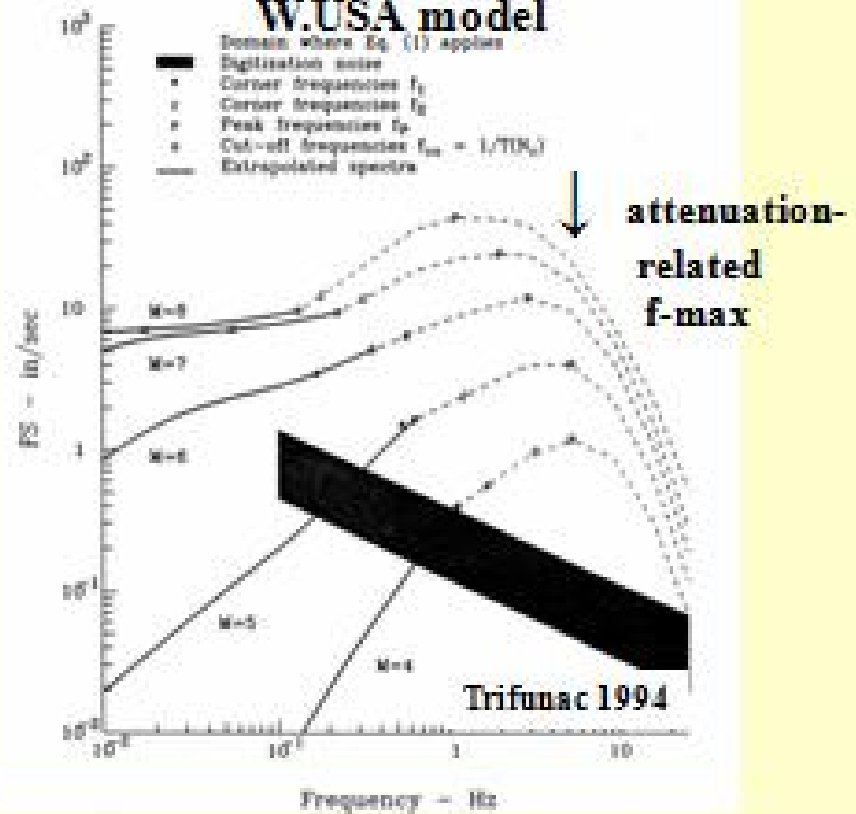
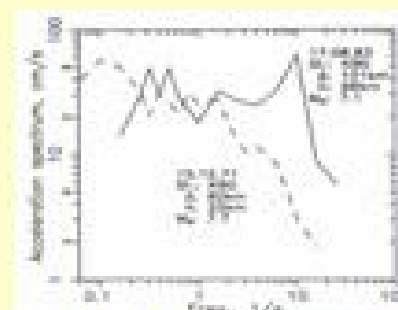
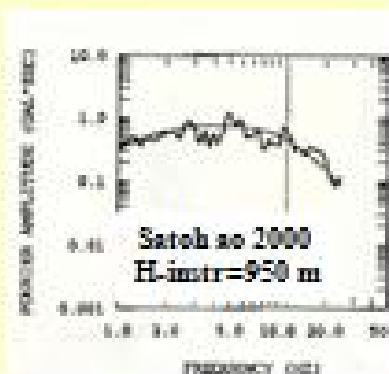
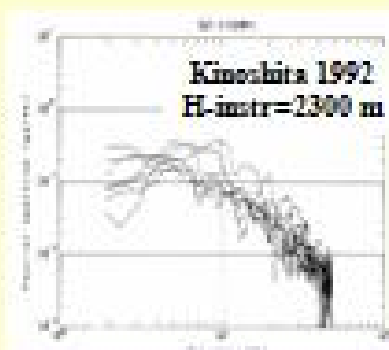


Illustration of features of observed acceleration spectra

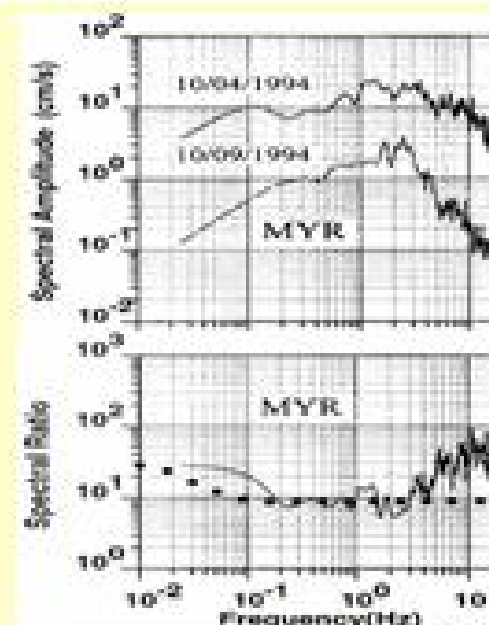
Source-related f_{max} : examples

Low to moderate magnitudes
 Instruments in deep boreholes, eliminated
 attenuation-related f_{max}
 Found, typically: source-related f_{max} between
 10 and 25 Hz,



Gusev a.o.
1997

Magnitudes 7-8
 Pairs of earthquakes recorded at the same station
 One of the two events have unusually low source-
 related $f_{max} \approx 3$ Hz
 Attenuation-related f_{max} is present as usual
 Can be eliminated by analyzing spectral ratio

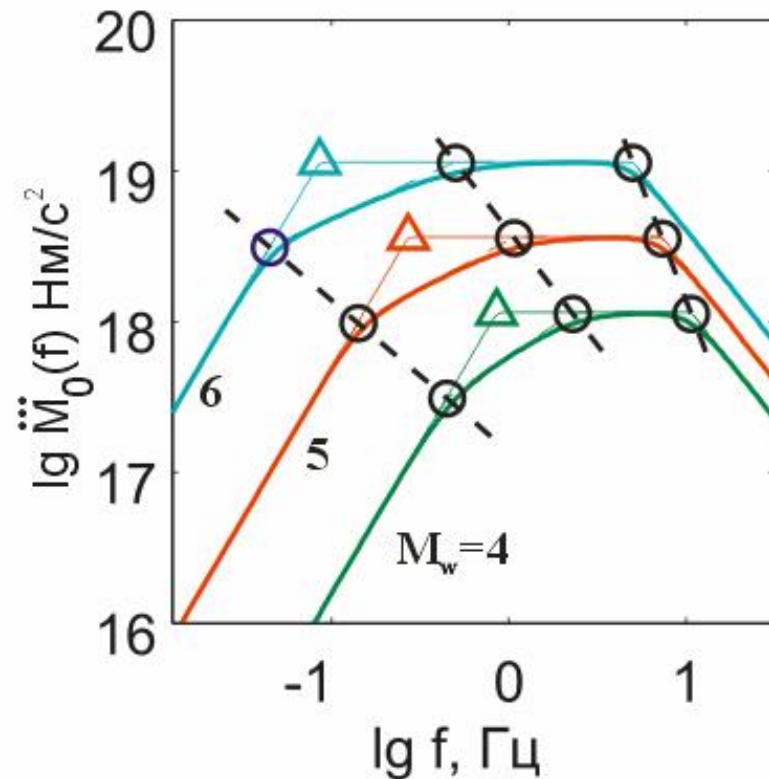
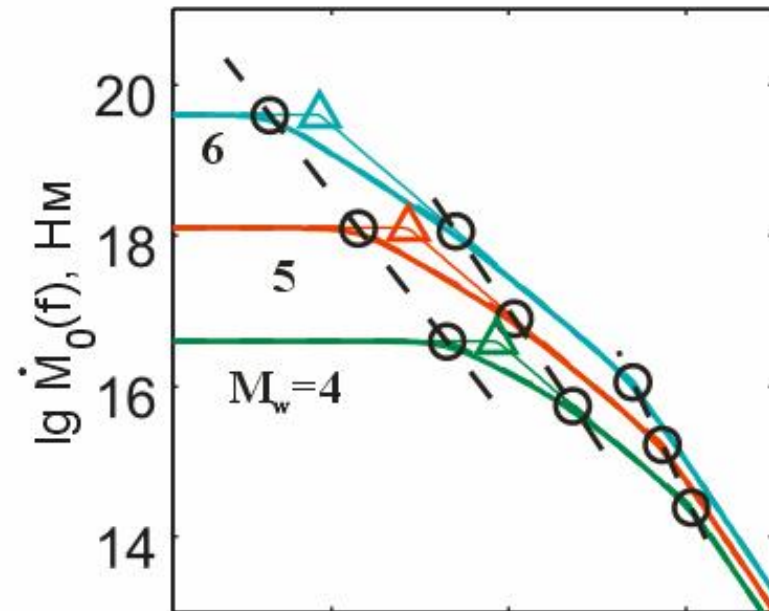


Sasatani 2001

Schematic of spectral scaling

with trends of fc_1 , fc_2 and fc_3

Note fc_0 (Δ): standard parameter
when data are analysed
based on Brune 1970 spectral
model.



“Source-controlled f_{max} ”,
or 3rd corner frequency,

f_{c3} :
does it exist?
how it scales?

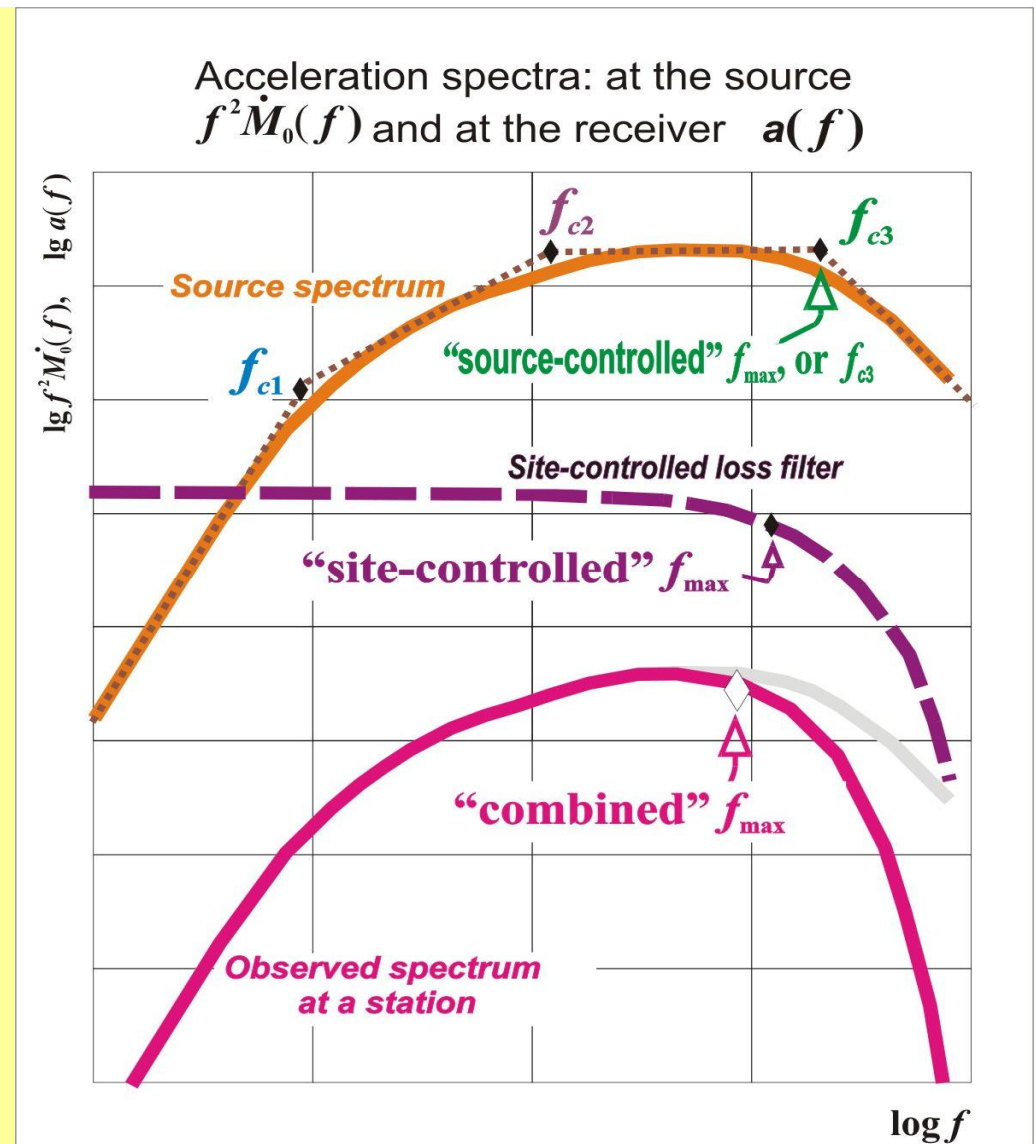
HISTORY

Hanks (1982) emphasized the “ f_{max} ”
phenomenon: $a(f)$ shows **HF cutoff**.

Papageorgiou and Aki(1983) and Gusev
(1983) ascribed it to **source**; Aki (1988)
noticed f_{max} vs M_0 trend with **unusual
scaling** that might support this idea

Hough and Anderson (1984) have shown
convincingly that **site-related loss**
controls f_{max}

Still, accumulated evidence suggests that
 f_{max} is a complex feature; it incorporates
both site-controlled and **source-**
controlled components



Outline of the study

1. Compile a preliminary attenuation model ($Q(f), \kappa_0$)
2. (a) Use it to correct observed spectra for propagation loss
(b) From corrected spectra, extract f_{c3} and also f_{c2}
3. Using the observed spectra within the limited $[f_{c2}, f_{c3}]$ frequency range, adjust the attenuation model
4. Repeat steps 2 and 3 until convergence
5. Discuss the obtained f_{c3} data set

Data set used

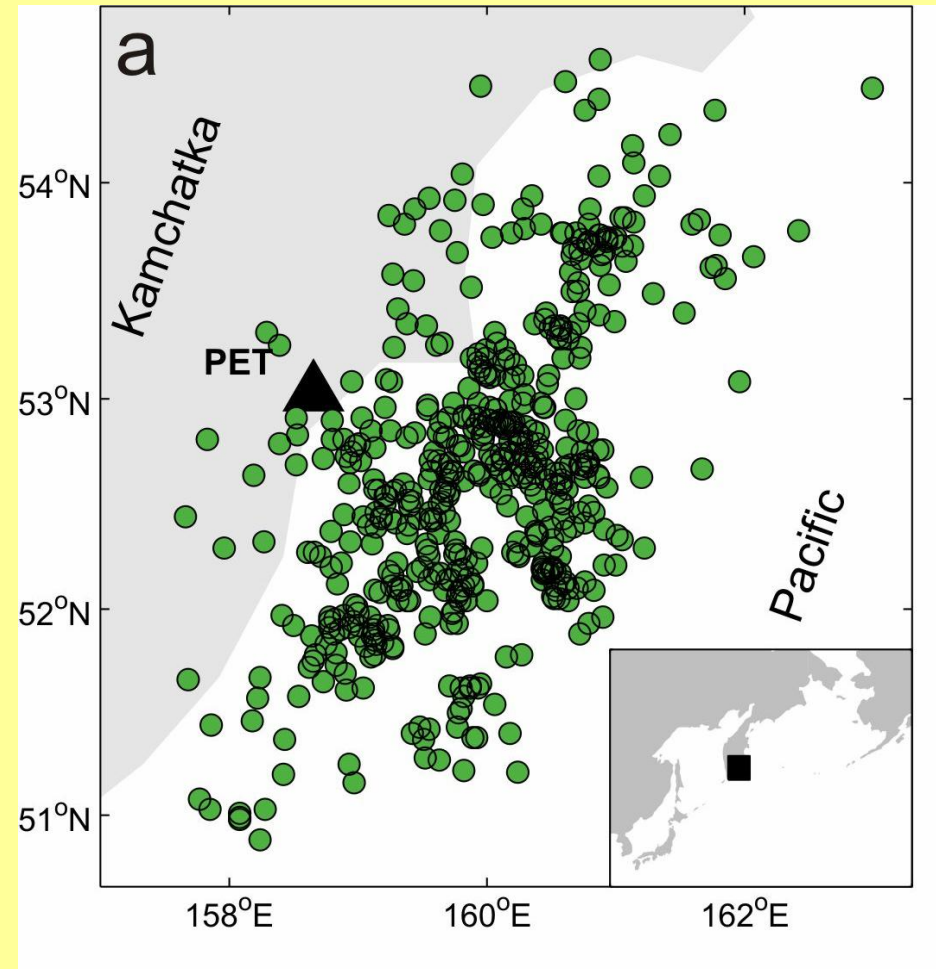
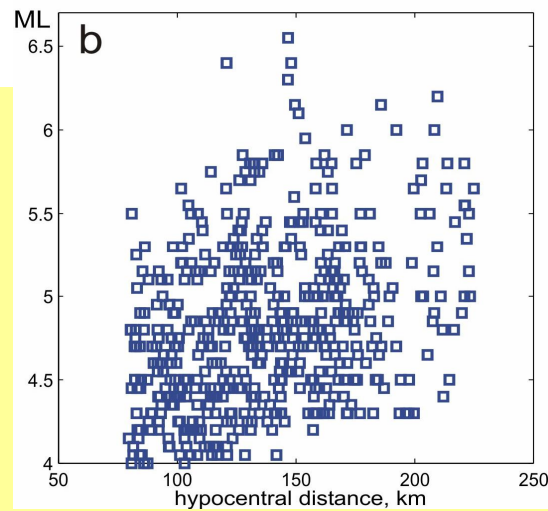
Records of **S-wave** group
by low-gain digital accelerograph
(HN channel, **80 sps**)
of IRIS BB station PET

439 records of 1993-2005
+ additional **130**

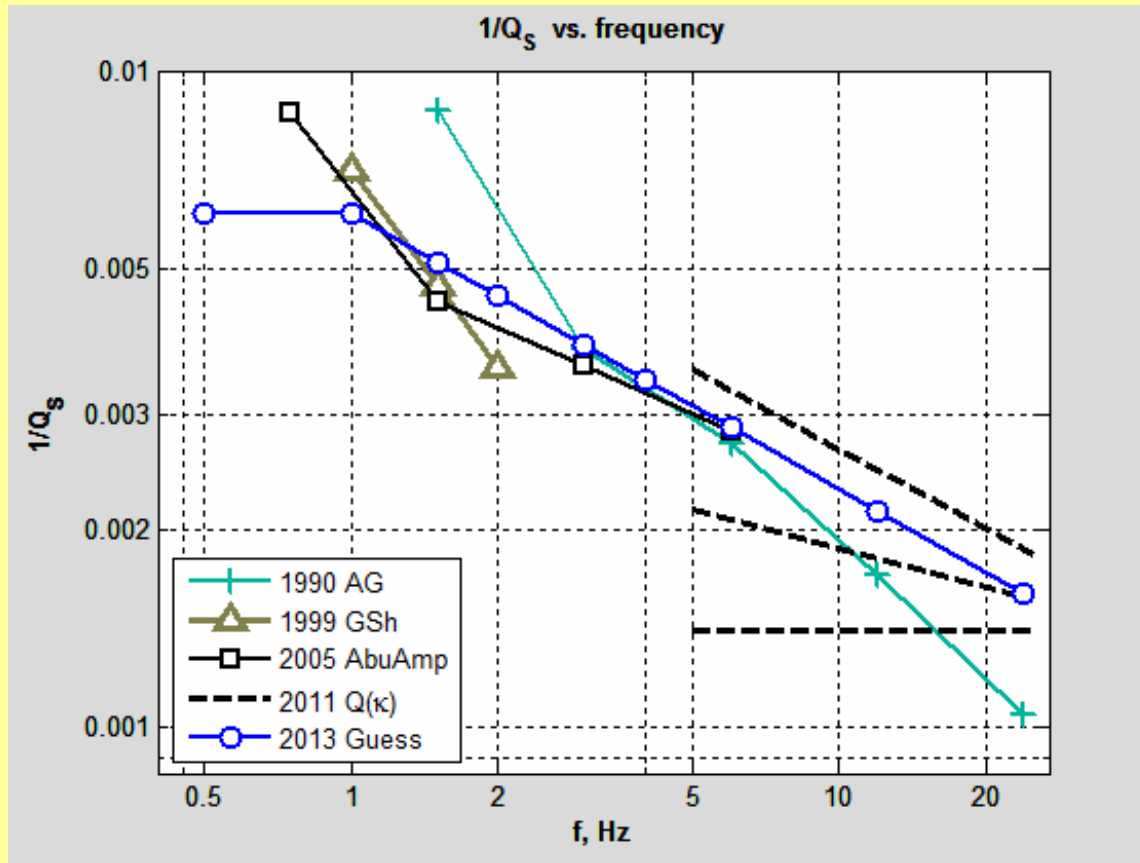
Hypo distance **80-220 km**

Depth range **0-200 km**,
mostly 0-50 km

$M_L = 4 - 6.5$



Compilation of the initial loss model on the basis of earlier results



accepted $Q_s(f)$ model: —————

Main sources used in compilation:

in the 1-6 Hz band from (Abubakirov 2005) who used coda-normalized spectral levels of band-filtered data

in the 5-25 Hz band based on (Gusev Guseva 2011) who analyzed kappa values;

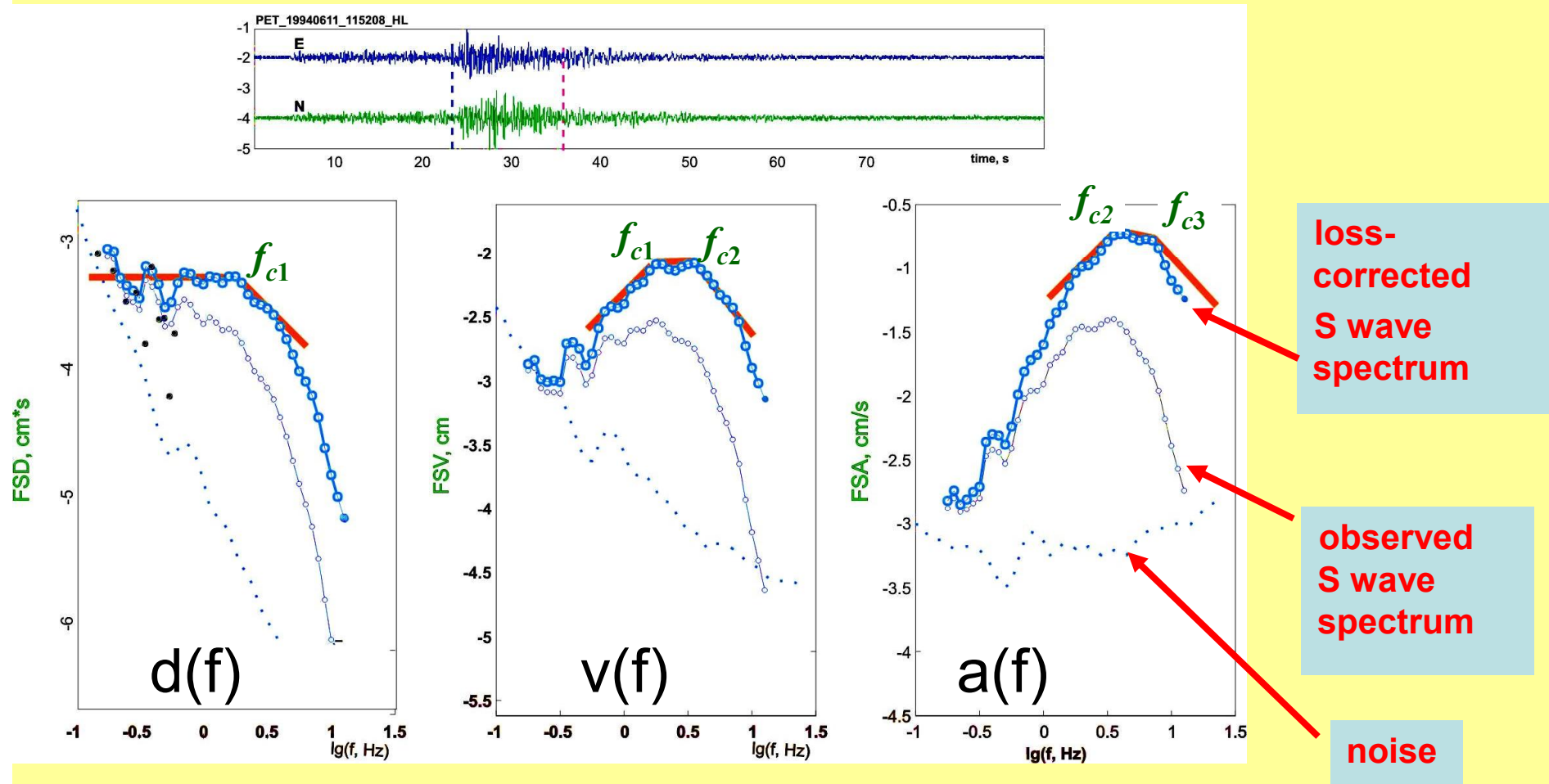
accepted trend at $r=100$ km:

$$Q_s(f) = 165 f^{0.42} \text{ —————}$$

also $\kappa_0 = 0.016$ s

and slow decay of Q_s^{-1} vs. r

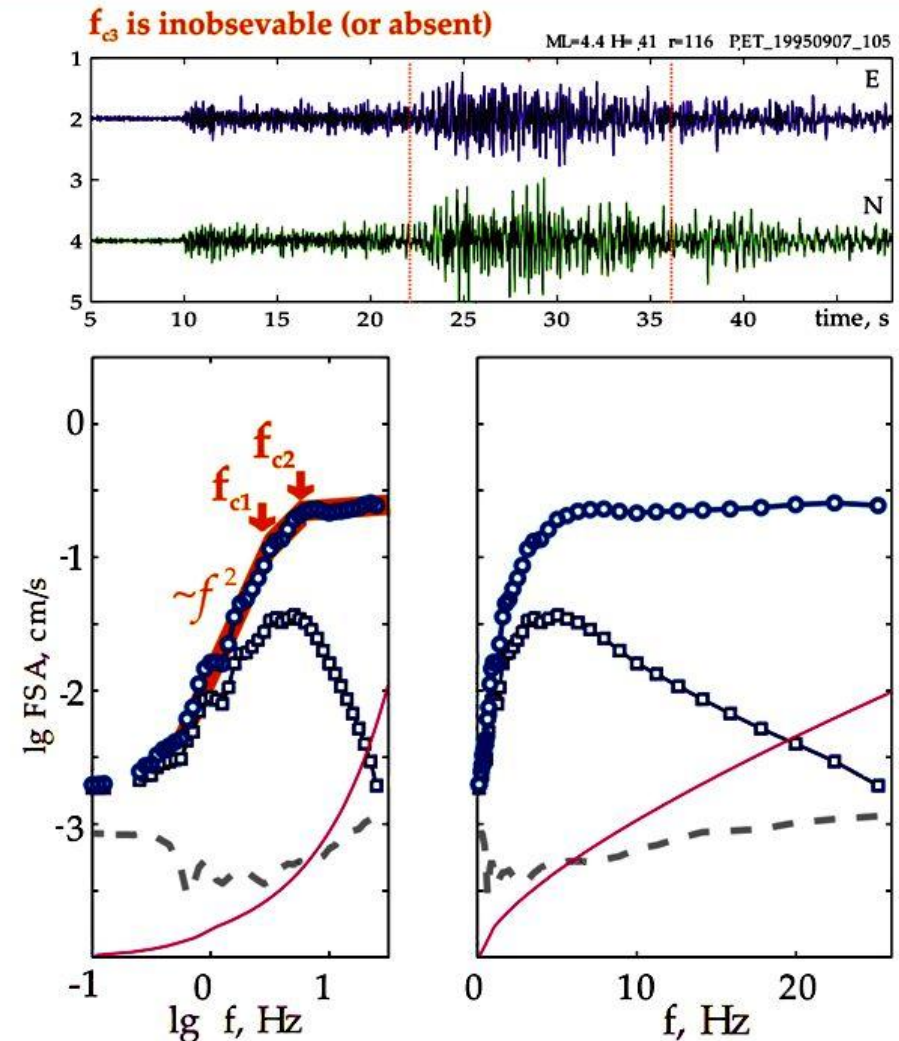
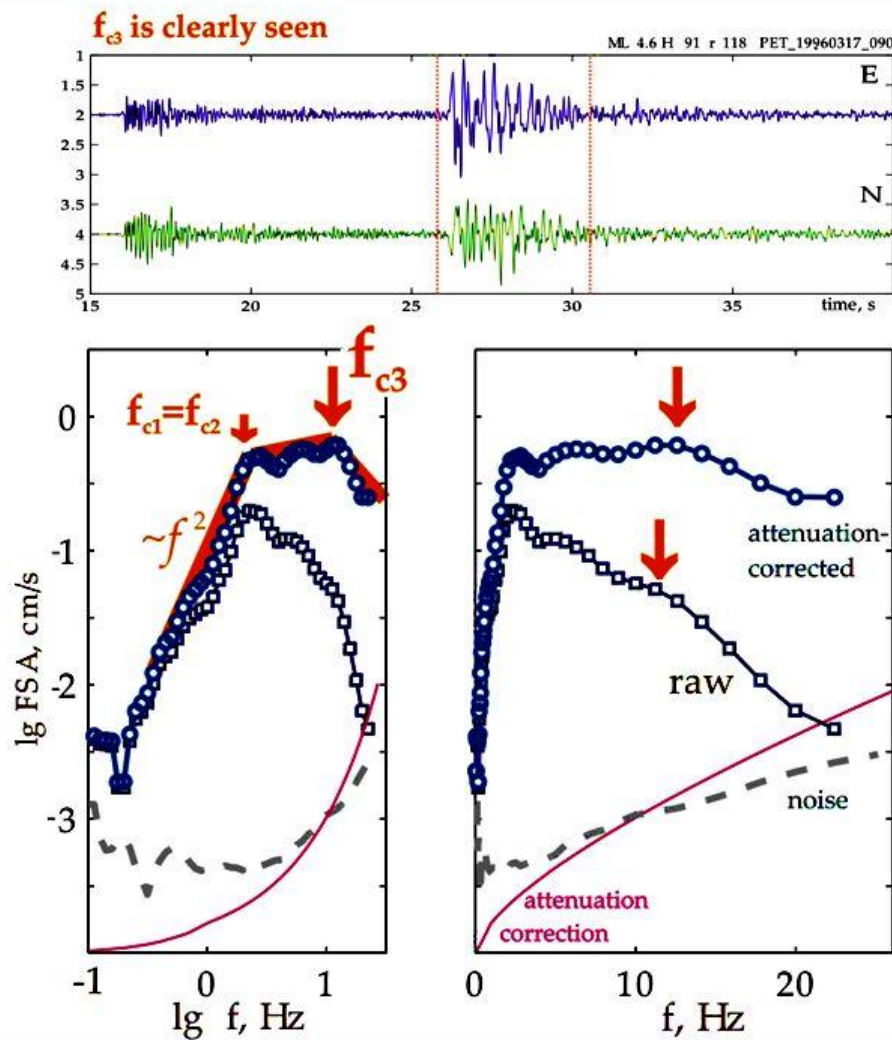
Example of processing in a case when each of f_{c1} , f_{c2} and f_{c3} is observable



spectral smoothing window used:
0.15 log units (1/2 octave)

when picking f_{ci} , slope of selected "plateaus"
in $v(f)$ and $a(f)$ plots was kept in the range ± 0.5

More example cases: f_{c3} may be observable or unobservable/absent



Here is why f_{c3} is difficult to notice when working in the log-linear scale

ITERATIVELY: find adjusted S-wave attenuation model using non-linear inversion.

Assumed attenuation model for loss factor in S-wave Fourier spectrum:

$$-\log_e \{A(f) / A_0(f)\} = \pi f \kappa_0 + \pi f(r/c)Q^{-1}(f, r)$$

where: r - hypocentral distance

κ_0 - constant loss factor for a site; $\kappa_0 \approx \ln 2 / \pi f_{\max\text{-loss}}$

c - wave velocity; and $Q(f,r)$ - path quality factor:

$$Q^{-1}(f, r) = Q_0^{-1} (f/f_0)^{-\gamma} (1 + q(r-r_0)/r_0)$$

where $f_0 = 1$ Hz, $r_0 = 100$ km, $c = 3.8$ km/c;

and **unknowns in inversion** are: κ_0, Q_0, γ, q

$Q_s(f|r=100\text{km}) :$

Guess 2013:

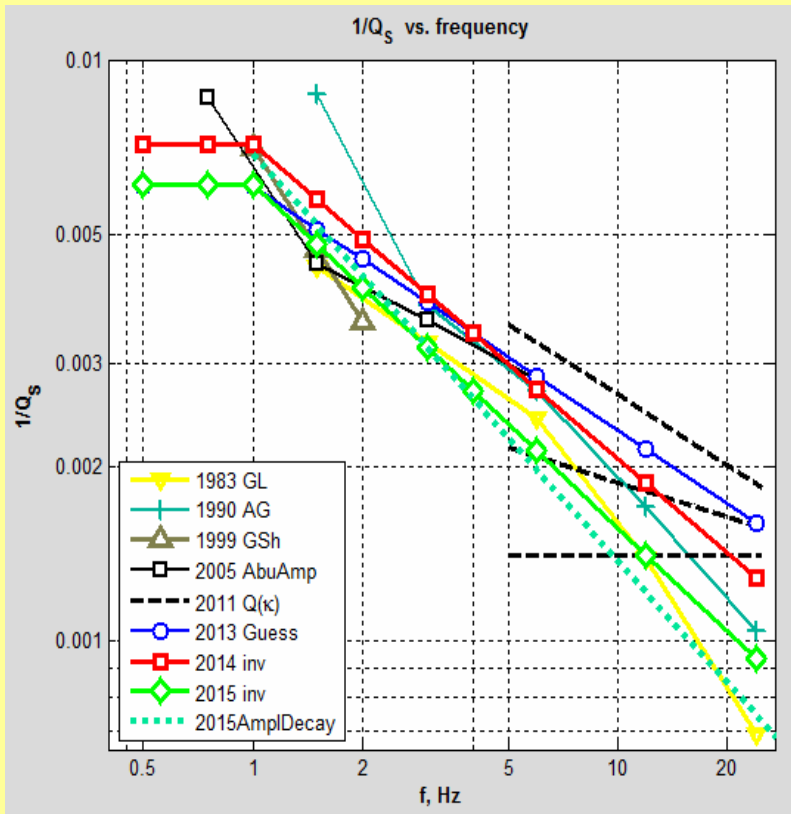
$$Q_s(f) = 165 f^{0.42} + \kappa_0 = 0.016 \text{ s}$$

Inverted 2014 (1st iteration):

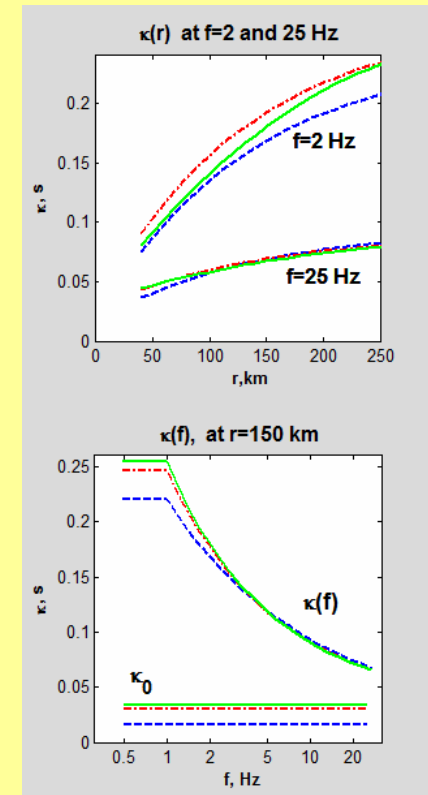
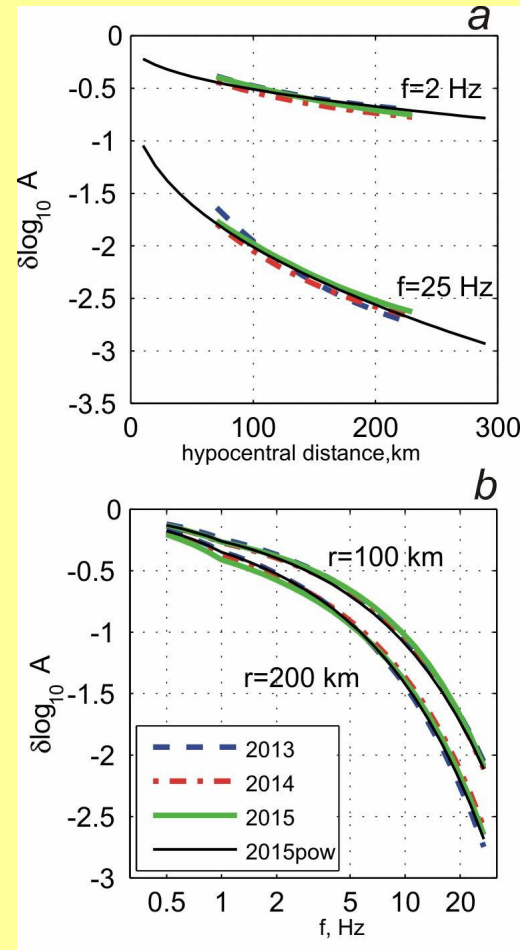
$$Q_s(f) = (140 \pm 33) f^{0.54 \pm 0.08} + \kappa_0 = 0.027 \pm 0.07 \text{ s}$$

Inverted 2015 (2nd iteration):

$$Q_s(f) = 164 f^{0.59} + \kappa_0 = 0.034$$

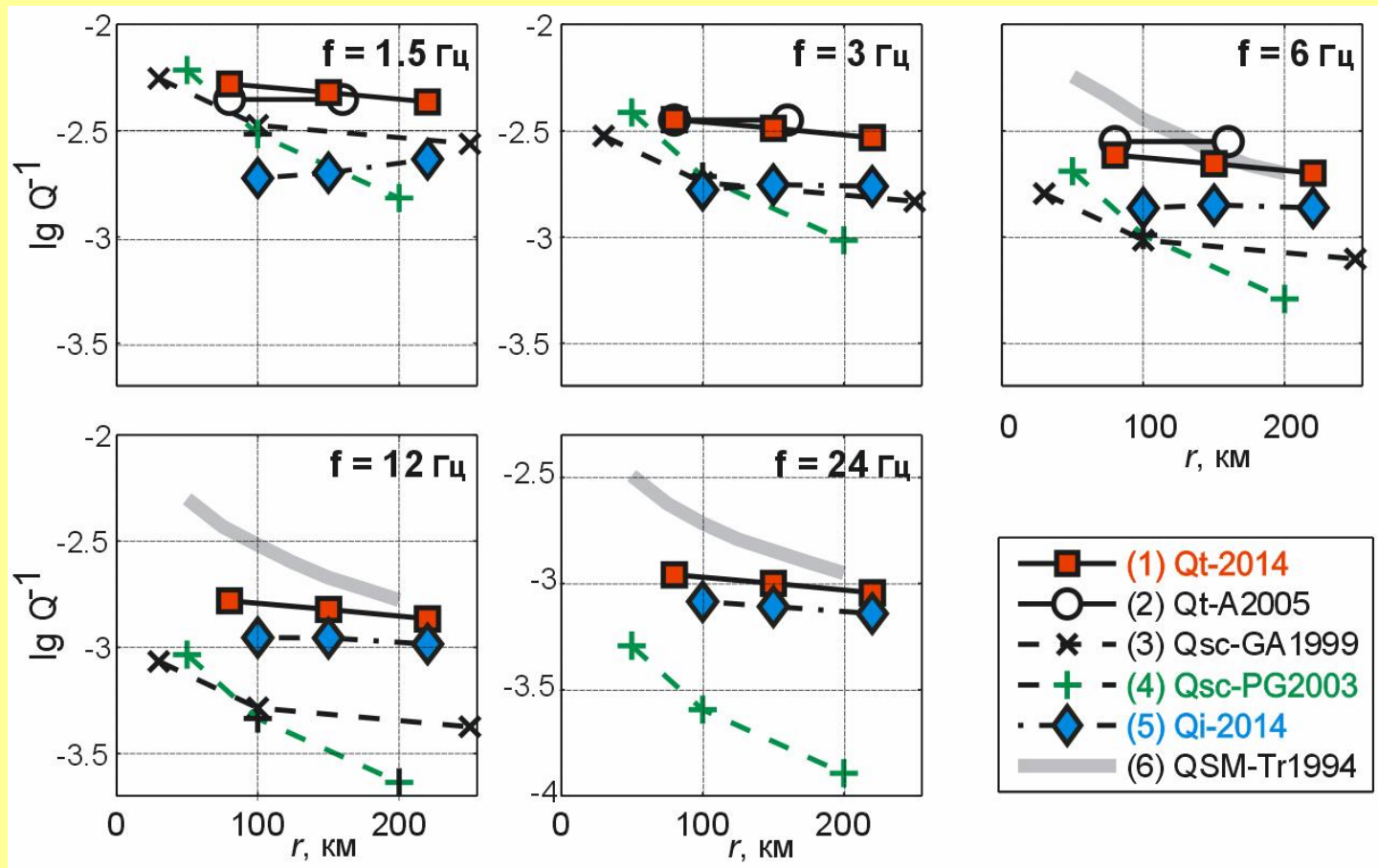


Comparing initial and inverted loss models

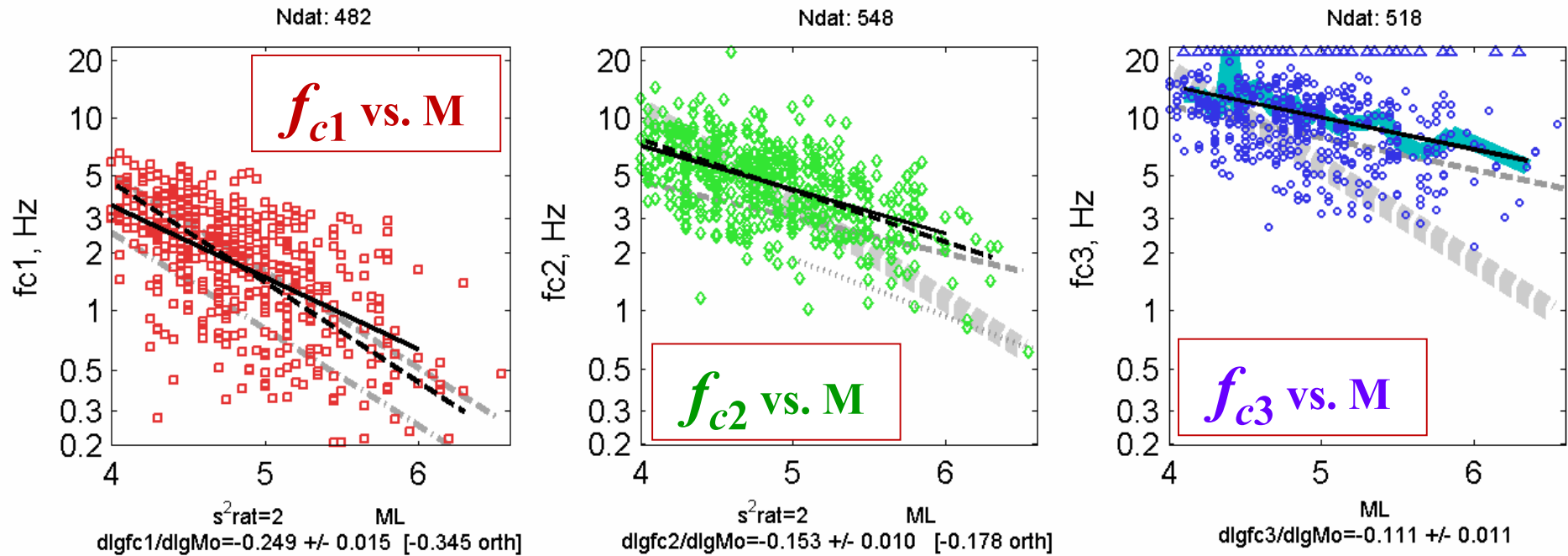


Loss variants **2014** and **2015** match
CONVERGENCE!

Attenuation: Q_{total} , $Q_{scattering}$ and $Q_{intrinsic}$



$f_{c1,2,3}$ trends side by side: see how scaling varies



(1) Each of the 3 trends is different

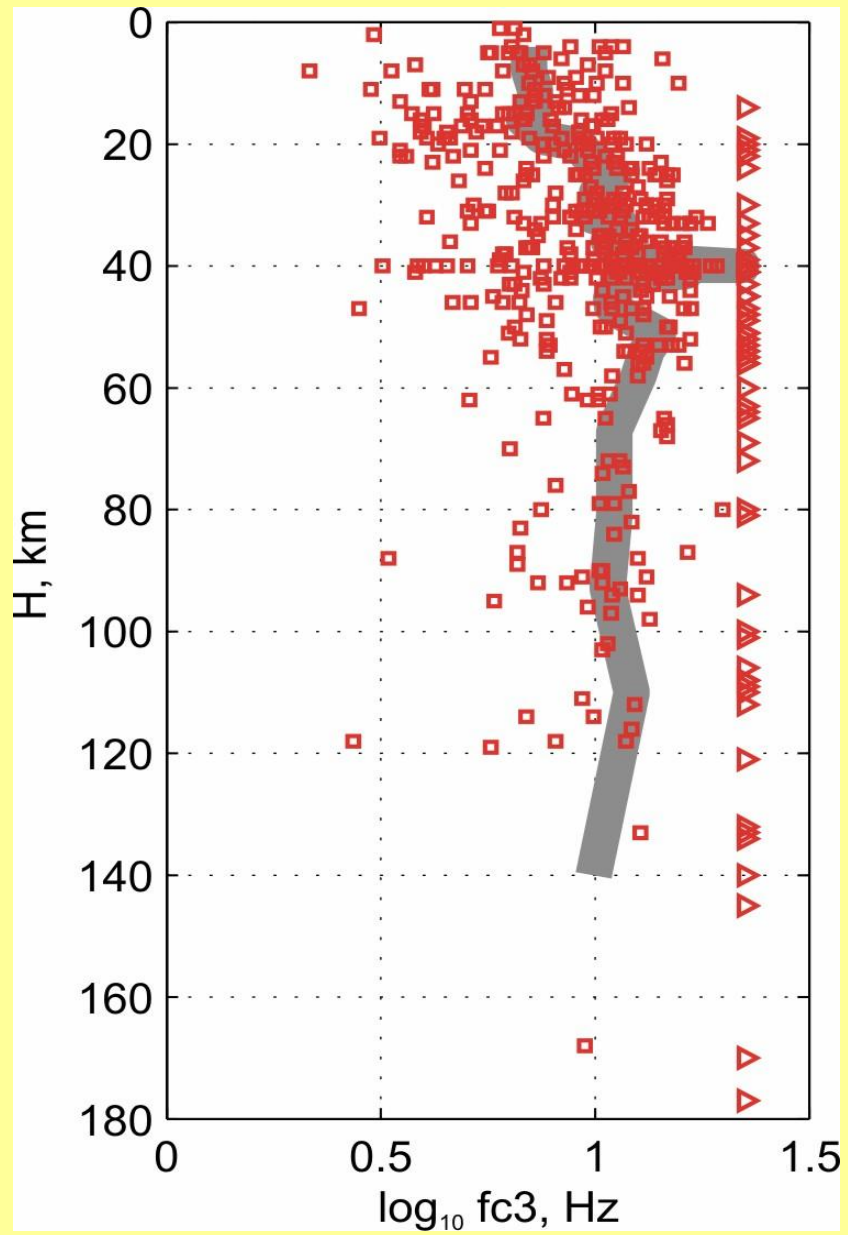
(2) Assumption of *similarity*:

\approx holds for f_{c1} ;

breaks for f_{c2} and f_{c3}

grey trends:

- (1) Taiwan, globe
- (2) ENA WUSA
- (3) Aki 1988



$$f_{c3}(H)$$

f_{c3}
grows
with
depth
up to
50 km

PART 2

Possible physics that underlies
the existence of f_{c3} and the trend of f_{c3} vs. M_0

Formation of f_{c3} can be attributed to the summary effect of the following

factors (probably complementary action):

- (1) lower (or high-wavelength) limit of the size
of fault surface heterogeneity [Gusev 1990]
- (2) finite fault zone thickness (gauge layer etc.) [Papageorgiou & Aki 1983]
- (3) finite cohesive zone width [Campillo 1983]

The trend $f_{c3} \propto f_{c1}^{0.2-0.3}$ or $f_{c3} \propto M_0^{-0.1}$

suggests that f_{c3} slowly decreases with source size

An underlying *cause* of such a trend may be
variations of maturity of fault surface :

the greater *distance* fault walls have slipped, the larger is their *wear*, and:

- (1) the lower is the upper cutoff of heterogeneity spectrum [by abrasion]
- (2) the wider/thicker is weak fault zone [by wear product accumulation]

[Gusev 1990; Matsu'ura 1990,1992].

Characteristic time hypothesis

- Introduce characteristic time of a fault surface:

$$T_{is} = T_{c3} = 1/f_{c3}:$$

it takes T_{is} for rupture to run distance $L_{is} \approx v_r * T_{is}$ where v_r – rupture velocity like 2.5-3.5 km/s. We assume $T_{is} \approx T_{c3} = 1/f_{c3}$.

- Also assume $T_{c1} = 1/f_{c1}$ near to rupture duration, and

- $T_{c2} = 1/f_{c2}$ near to local rise time of slip

Dimensionless description of a fault

- let $\tau_1 = T_{c1} / T_{c3} = f_{c3} / f_{c1}$, be normalized rupture duration,
- and $\tau_2 = T_{c2} / T_{c3} = f_{c3} / f_{c2}$ be normalized rise time
- then key dependence is $\tau_2 = \tau_2(\tau_1)$.
- also one can set normalized rupture velocity as unity, then normalized rupture size is $\lambda_1 = \tau_1$;

Dependence of f_{c1} , f_{c2} and f_{c3} on M_0 .

for f_{ci} , define

$$\alpha_i = -d \lg f_{ci} / d \lg M_0$$

Orthogonal regression
gives, for $fc1$:

$$\alpha_1 = 0.315 \pm 0.019,$$

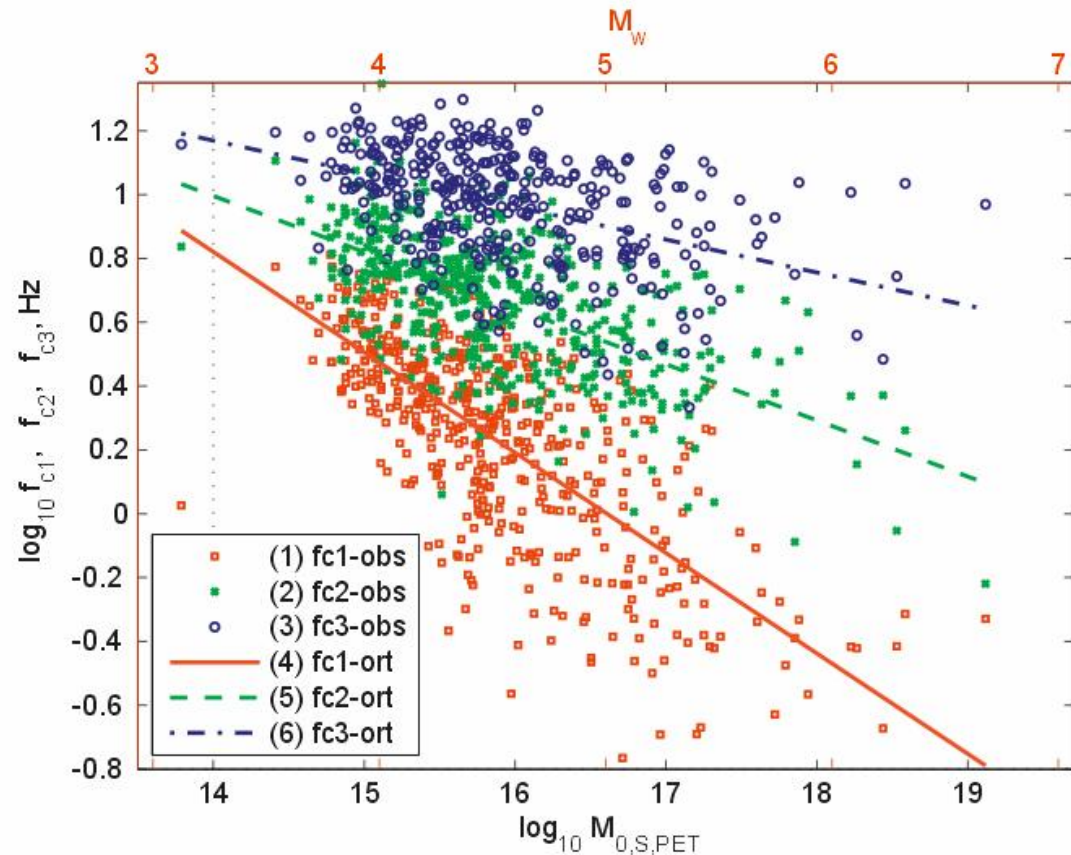
(near to similarity that predicts $\alpha_1 = 1/3$);

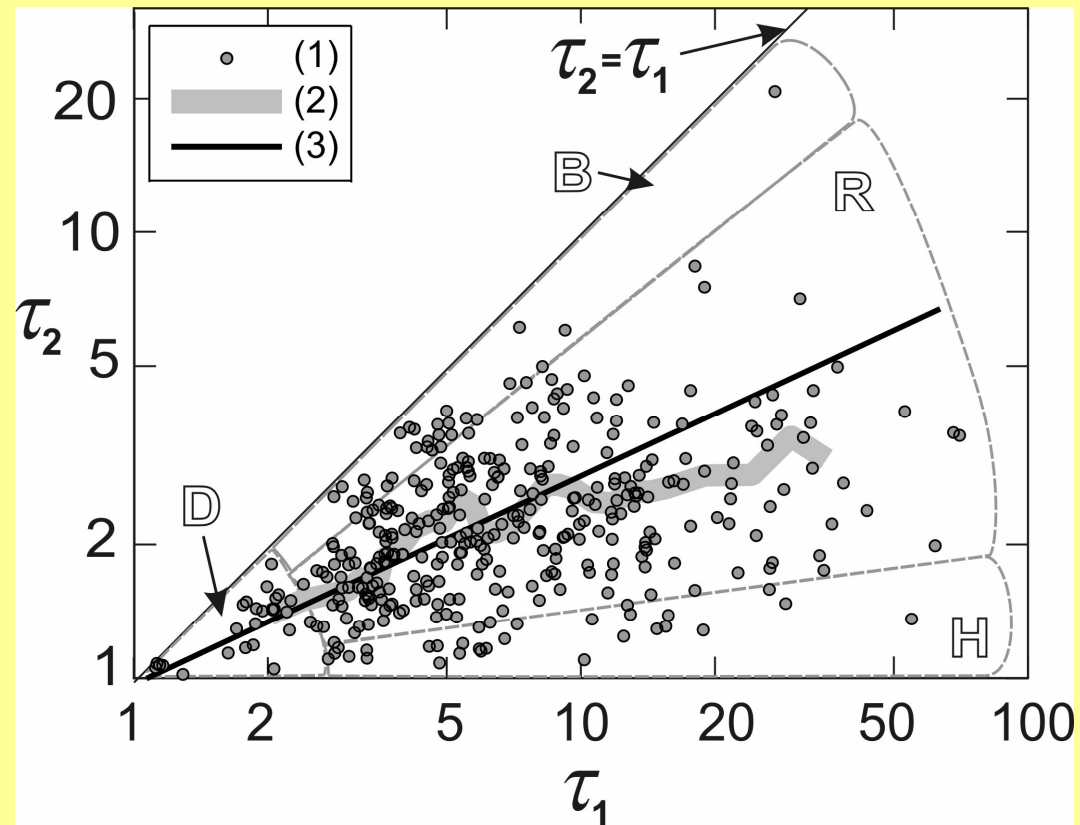
Also:

$$\alpha_2 = 0.176 \pm 0.017 \text{ and}$$

$$\alpha_3 = 0.103 \pm 0.025.$$

Both show significant break
of similarity.





Individual values of τ_1 and τ_2 for 430+ Kamchatka data

- Zone B: Brune1970 style, $L \approx W$
- Zone H: Haskell 1964 style, $L \gg l$
- Zone D: Kostrov 1964-Dahlen 1974 style (ω^{-3} spectrum)
- Zone R: regular behavior:

There are analogies in many fields that study stochastic modes of

- interface motion
- growth of solid: atoms, suspended particles etc
- growth of lichen, cancer, etc
- fire fronts
- deflagration (burning front in gas)
- imbibition (wetting, blotting)
- ferromagnetic domain wall motion
- crack edge propagation

in all these phenomena, rough, often fractal (self-similar) lines are formed

Rough interfaces in disordered media



Burned paper



Ink in paper



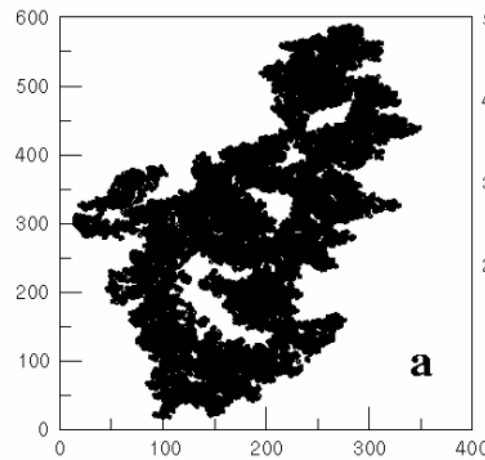
Lichen



Bacterium colony



Torn paper



Forest fire,
from satellite image

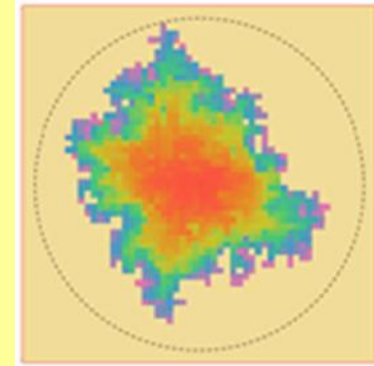


Fig. 4. Horizontal projection of the cluster of model B ($p = 0.8009 - p_c$) which was started at the center of the screen 2^7 time steps ago. The current diameter of the cluster is about 2^7 . The blue area shows the flat interface that is left dry since the beginning of the process. Darkest shades of gray correspond to the largest heights of the interface. Red dots forming "fractal dust" indicate cells that become wet at the current time step.



REAL

- Bonami 2008
- Buldyrev et al 1993
- Caldarelli 2001
- Gouyet 2005
- Halpin-Healy 1995
- Schmittbuhl et al 2003

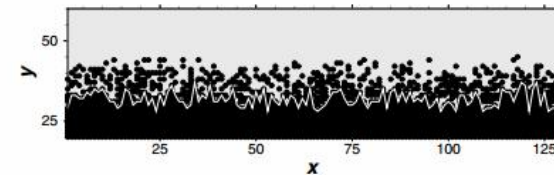
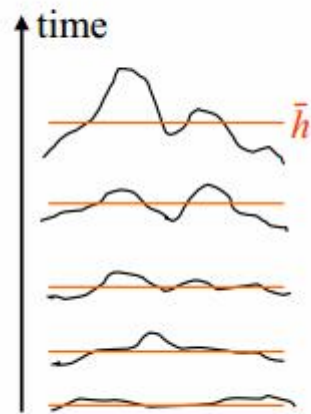


FIG. 1. The crack front for a 128×128 system. The fracture is propagating from bottom to top. The broken springs are black dots. The crack front is drawn as a white line.

SIMULATED

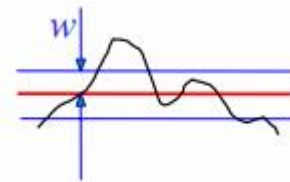
Analysis of rough edges



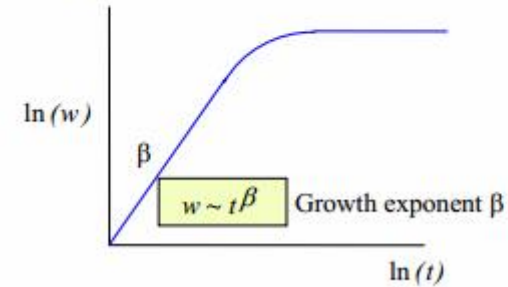
$$\bar{h}(t) := \frac{1}{L} \sum_{i=1}^L h(i, t)$$

$$\bar{h}(t) \sim t$$

Growth exponent



$$w(L, t) = \sqrt{\frac{1}{L} \sum_{i=1}^L [h(i, t) - \bar{h}(t)]^2}$$



growth exponent β

defined by :

rms width \propto time ^{β}

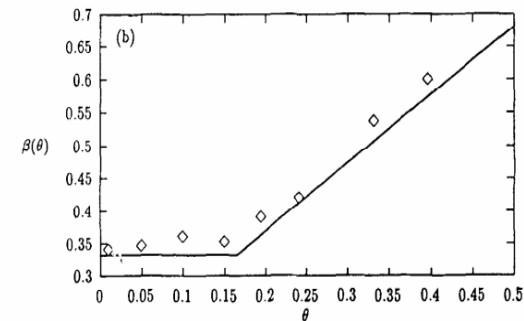
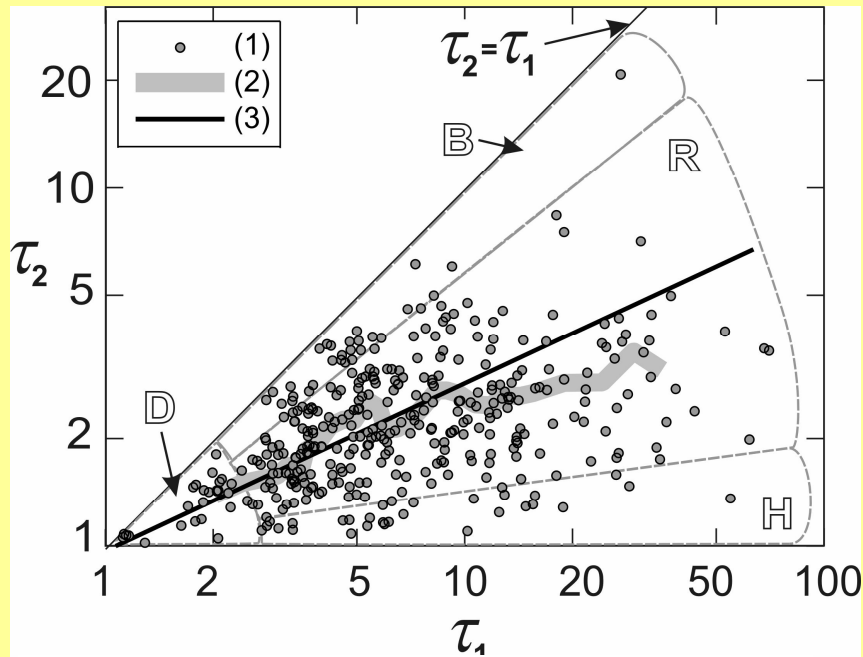


Fig. 4.18. Ballistic deposition subject to temporally correlated noise [LSW92], simulation results for (a) saturation width exponent $\chi = \alpha$, and (b) early-time index β .



Slope of orthogonal regression line:
 $\beta = 0.47 \pm 0.043$.

Slope β of rms width vs time trend

$$\beta = -d \lg \tau_2 / d \lg \tau_1$$

| | β |
|----------------------------------------------------|---------|
| <i>$\tau_2(\tau_1)$ earthquake data</i> | |
| Kamchatka, individual data | 0.47 |
| Kamchatka, <i>trends</i> | 0.34 |
| W.USA etc Aki 1988, <i>trends</i> | 0.57 |
| Middle Asia, <u>Rautian data, trends</u> | 0.42 |
| <i>Theoretical models</i> | |
| Eden growth | 1/3 |
| Directed percolation <u>depinning</u> | 0.65 |
| <i>Observed trends</i> | |
| Crack in PMMA | 0.55 |
| paper burning | 0.47 |
| superconductor transformation front | 0.65 |
| <u>imbibition</u> | 0.60 |

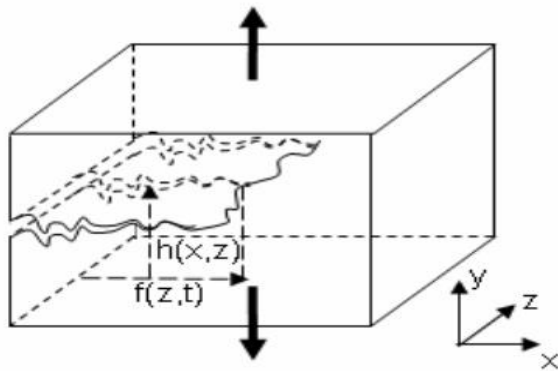
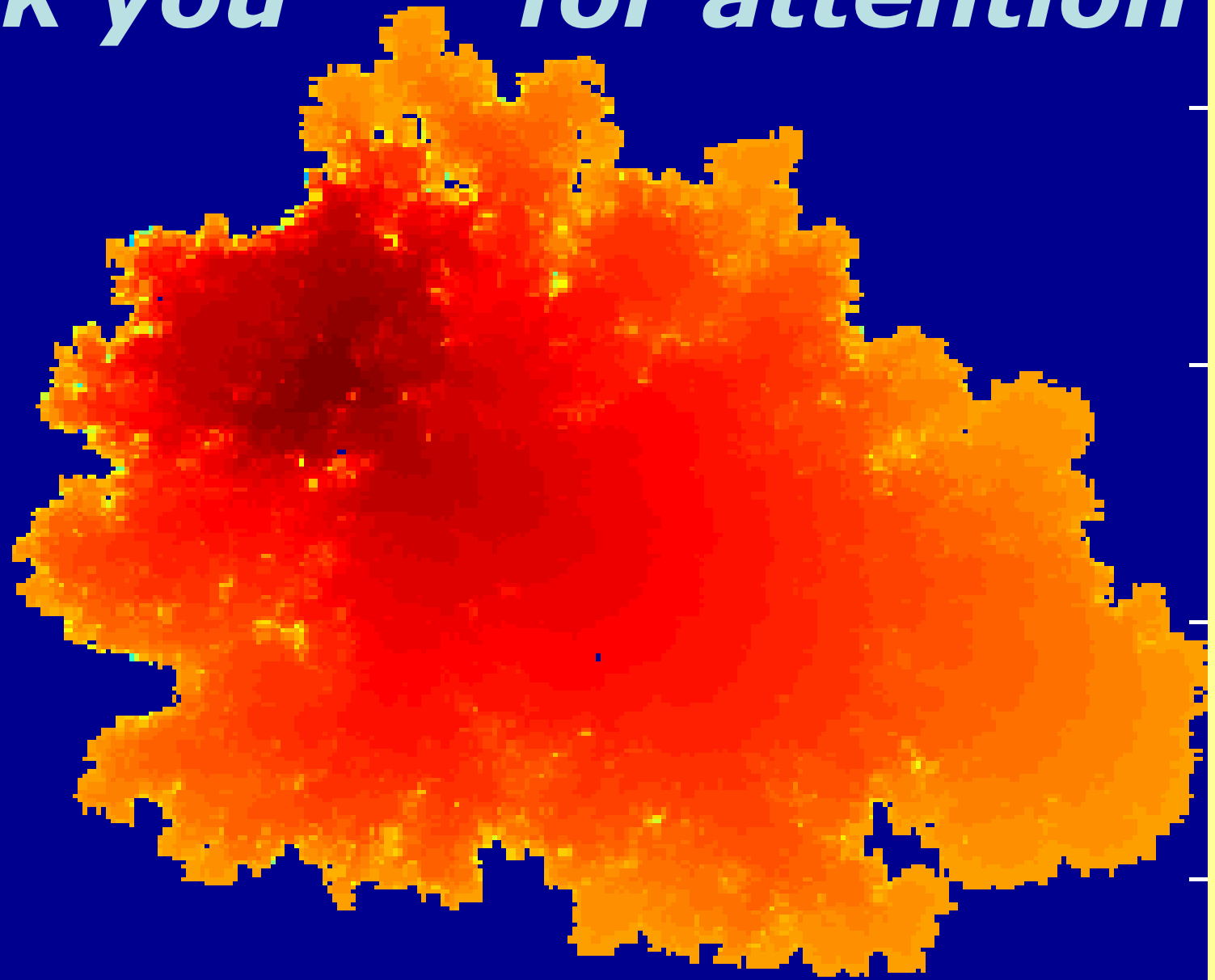


Figure 14. Sketch and notation of a crack front propagating in a 3D material.

point of growth!

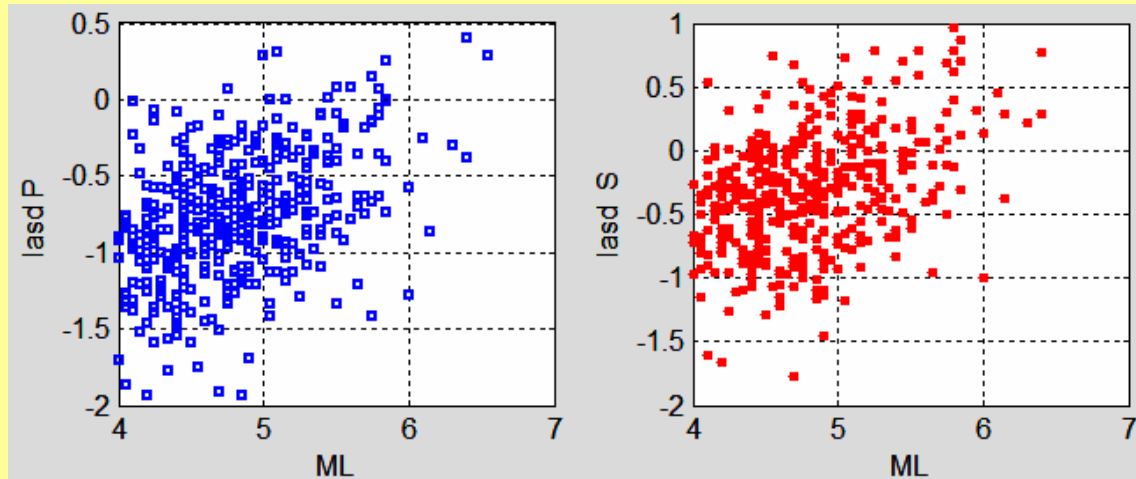
thank you

for attention



thank you for attention

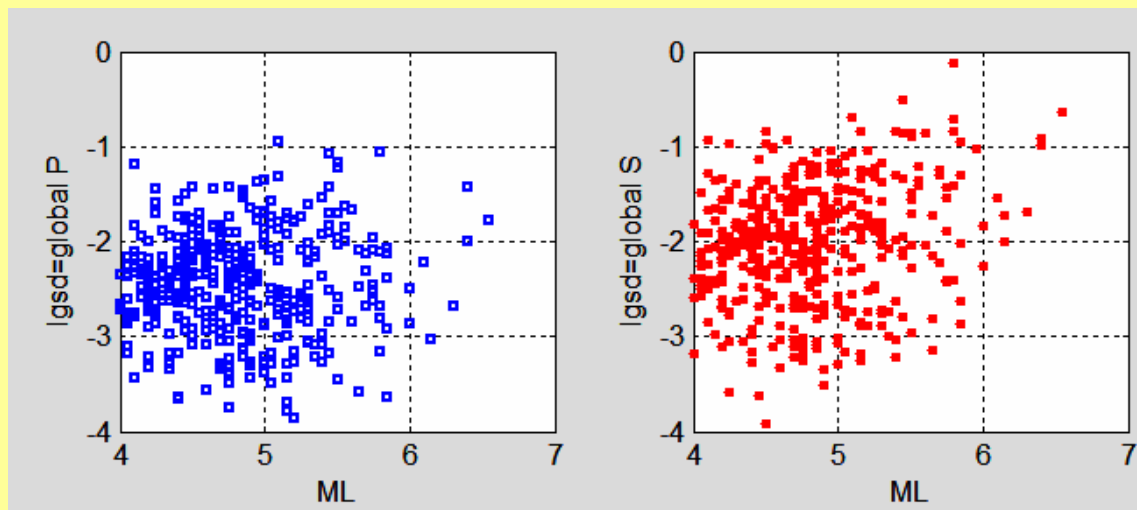
Apparent stress σ_a vs M : no similarity



Two ways of checking the similarity assumption make different results

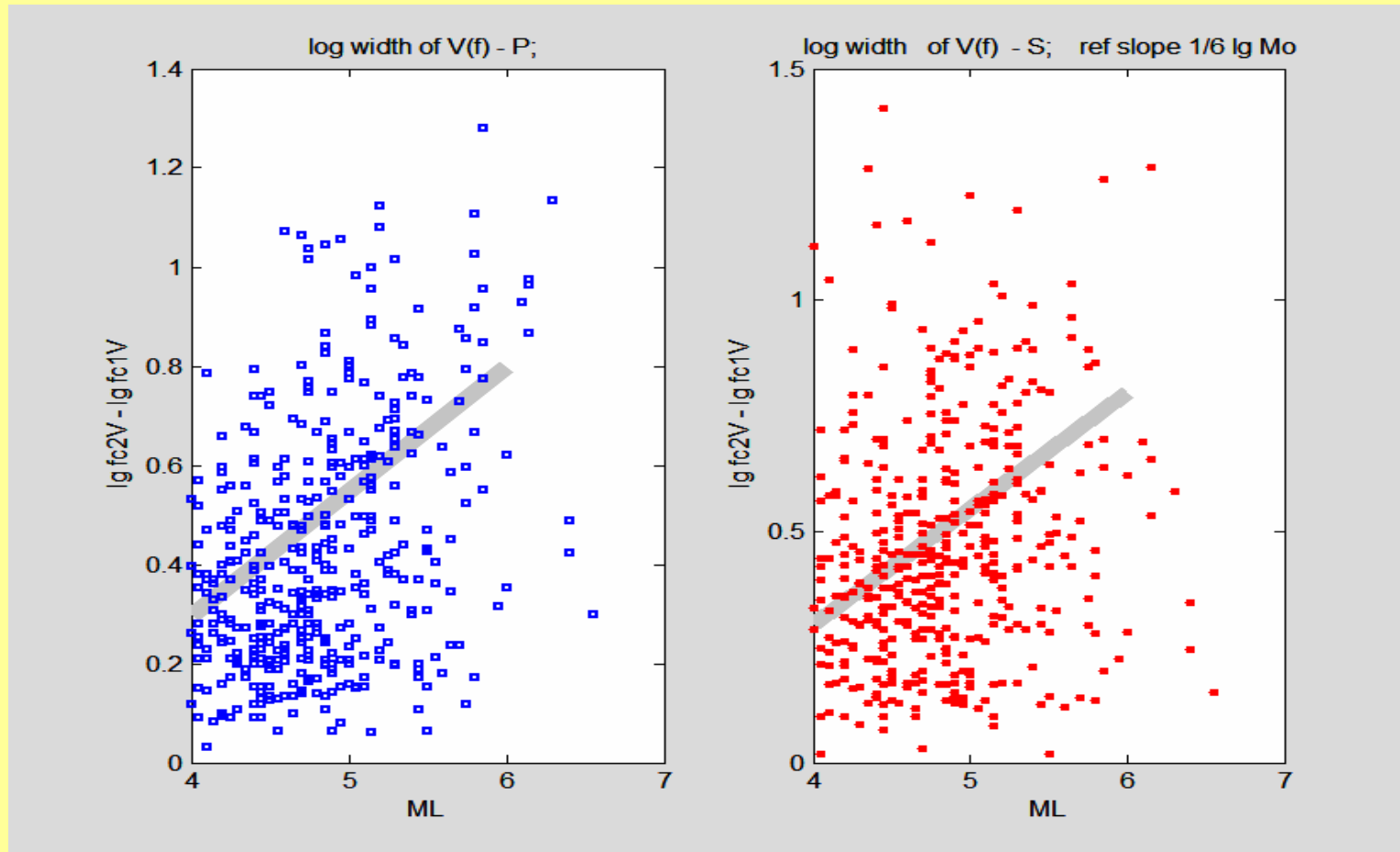
$$\sigma_a = \frac{E_s}{M_0} \propto \frac{v_{\max}^2(f)(f_{c2} - f_{c1})}{d(f)|_{f=0}}$$

Stress drop $\Delta\sigma$ vs. M : approximate similarity



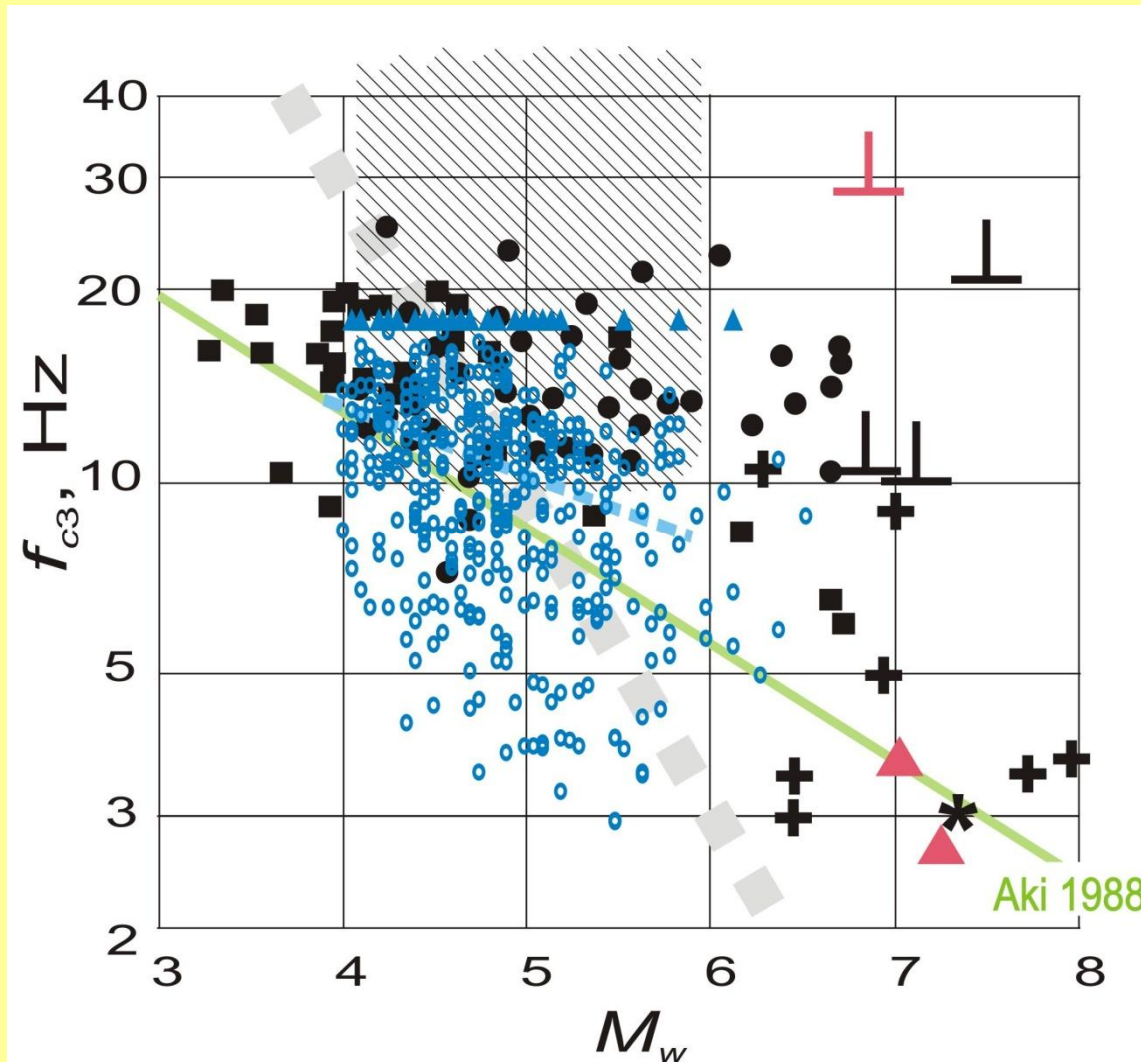
$$\Delta\sigma \approx \frac{M_0}{R^3} \propto f_{c1}^3 \cdot d(f)|_{f=0}$$

$LV = \log f_{c2} - \log f_{c1}$: log-width of velocity spectrum $V(f)$ vs. M
 (similarity would result in M -independent LV)



Variation of LV with M causes M -dependence of σ_a at a fixed $\Delta\sigma$

Trend of f_{c3} vs. M_w : new data compared to compilation-2010



black: compilation
[Gusev 2013]

○ ▲ 2015 Kamchatka
data

— Aki 1988

▲ ⊥ Faccioli 1986

High f_{c3} :

NO ANOMALY

**An important part of
the general picture**